Baryon-strangeness correlations in Au+Au collisions at $\sqrt{s_{NN}} = 7.7$–200 GeV from the UrQMD model

Zhenzhen Yang (杨贞贞),[1] Xiaofeng Luo (罗晓峰),[1,*] and Bedangadas Mohanty[2]

[1]*Key Laboratory of Quark and Lepton Physics (MOE) and Institute of Particle Physics, Central China Normal University, Wuhan 430079, China*

[2]*School of Physical Sciences, National Institute of Science Education and Research, HBNI, Jatni 752050, India*

(Received 24 October 2016; published 30 January 2017)

Fluctuations and correlations of conserved charges are sensitive observables for studying the QCD phase transition and critical point in high-energy heavy-ion collisions. We have studied the centrality and energy dependence of mixed cumulants (up to fourth order) between net baryon and net strangeness in Au + Au collisions at $\sqrt{s_{NN}} = 7.7$, 11.5, 19.6, 27, 39, 62.4, and 200 GeV from the ultrarelativistic quantum molecular dynamics (UrQMD) model. To compare with other theoretical calculations, we normalize these mixed cumulants by various order cumulants of net-strangeness distributions. We found that the results obtained from UrQMD calculations are comparable with the results from lattice QCD at low temperature and hadron resonance gas model. The ratios of mixed cumulants ($R_{11}^{BS}, R_{13}^{BS}, R_{22}^{BS}, R_{31}^{BS}$) from UrQMD calculations show weak centrality dependence. However, the mixed-cumulant ratios R_{11}^{BS} and R_{31}^{BS} show strong increase at low energy, while the R_{13}^{BS} and R_{22}^{BS} are similar at different energies. Furthermore, we have also studied the correlations between different hadron species and their contributions to the net-baryon and net-strangeness correlations. These model studies can provide baselines for searching for the signals of QCD phase transition and critical point in heavy-ion collisions.

DOI: 10.1103/PhysRevC.95.014914

I. INTRODUCTION

Fluctuations and correlations of the conserved charges have been proposed to be sensitive observables to study the QCD phase transition and critical point (CP) in relativistic heavy-ion collisions [1–4]. Theoretical calculations show that fluctuations and correlations of conserved charges are distinctly different in the hadronic and quark-gluon plasma (QGP) phases [5]. In the deconfined state of quarks and gluon, the elementary set of conserved charges is given by the corresponding quark flavors: net upness ($\Delta u = u - \overline{u}$), net downness ($\Delta d = d - \overline{d}$), and net strangeness ($\Delta s = s - \overline{s}$) [6–9]. In hadronic state the conserved charges are net baryon (B), net charge (Q), and net strangeness (S). Recently, Lattice QCD calculations have shown that various order (up to fourth order) net-strangeness (S) fluctuations and their correlations with net charge (Q) and net baryon (B) are quite sensitive to the quark-hadron phase transition [9].

In the years 2010–2014, Relativistic Heavy Ion Collider (RHIC) has completed the first phase of the beam energy scan (BES) program [10]. In this program the the collision energies in Au + Au collisions were tuned to explore the QCD phase structure at high baryon density [11–13]. The STAR experiment at RHIC has collected Au + Au collision data with $\sqrt{s_{NN}} = 7.7$, 11.5, 14.5, 19.6, 27, 39, 62.4, and 200 GeV. One of the experimental motivations is to measure the correlations between net baryon and net strangeness with these experimental data collected to study the QCD phase transition in heavy-ion collisions [14]. To provide baselines for the correlation measurements to study the phase transition, we have calculated these observables in Au + Au collisions at RHIC BES energies with the ultrarelativistic quantum molecular dynamics (UrQMD) model and compared them to the model results from lattice QCD and hadron resonance gas model. In addition, given that at lower energies we expect to see the effect of baryon stopping and associated production of strangeness, we have also studied the contributions of various hadron species to the baryon-strangeness correlations.

The paper is organized as follows. In the next section, we briefly review fluctuations and correlations of conserved charges in hadronic and quark-gluon plasma states and give the corresponding results from hadronic resonance gas model and lattice QCD. In Sec. III, we present the mixed-cumulant ratios of net baryon and net strangeness and also discuss the contribution of strange baryons to the baryon-strangeness correlations in Au + Au collisions at RHIC BES energies from the UrQMD model. Then, we give a brief summary in Sec. IV. Finally, we present as an appendix the statistical error calculations for various order mixed cumulants.

II. THE UrQMD MODEL

The UrQMD model [15,16] is based on a microscopic transport theory where the phase-space description of the reactions is considered. It treats the propagation of all hadrons on classical trajectories in combination with stochastic binary scattering, color string formation, and resonance decay. It incorporates baryon-baryon, meson-baryon, and meson-meson interactions; the collisional term includes more than 50 baryon species and 45 meson species. The model preserves the conservation of electric charge, baryon number, and strangeness number as expected for a QCD matter. It also models the phenomena of baryon stopping, an essential feature encountered in high-energy heavy-ion collisions at lower beam energies. The model does not include quark-hadron phase

*xfluo@mail.ccnu.edu.cn

transition or the QCD critical point. It can simulate heavy-ion collisions in the energy range from SIS (SchwerIonen Heavy-ion Synchrotron) to Relativistic Heavy Ion Collider (RHIC) and even for the heavy-ion collisions at the Large Hadron Collider (LHC) [17–19]. In this model, the space-time evolution of the fireball is studied in terms of excitation and fragmentation of color strings and formation and decay of hadronic resonances. The comparison of the data (this paper deals with B-S correlations) onto those obtained from the UrQMD model will tell about the contribution from the hadronic phase and its associated processes.

III. OBSERVABLES

In statistics, the generating function of mixed cumulants for random variables, X_1, X_2, ..., $X_n (n > 2)$ are defined as

$$G(t_1,t_2,\ldots,t_n) = \log\left\langle e^{\sum_{i=1}^{n}(t_j X_j)}\right\rangle. \tag{1}$$

Then, the mixed cumulants of random variables $X_1, X_2, \ldots, X_n (n > 2)$ can be expressed as [20]

$$\begin{aligned} &C(X_1,X_2,\ldots,X_n) \\ &= \sum_{\pi}(|\pi|-1)!(-1)^{(|\pi|-1)}\prod_{C\in\pi}E\left(\prod_{i\in C}X_i\right) \\ &= \sum_{\pi}(|\pi|-1)!(-1)^{(|\pi|-1)}\prod_{C\in\pi,|C|\geqslant 2}E\left(\prod_{i\in C}\delta X_i\right), \end{aligned} \tag{2}$$

where π runs through the list of all partitions of $1,2,\ldots,n$, C runs through the list of all blocks of partitions π, $|\pi|$ is the number of parts in the partition, and $|C|$ is the number of parts in the block C.

In mixed-cumulants analysis, we use B and S to represent the net-baryon number and net-strangeness in one event, respectively. The average values over whole event ensemble are denoted by $\langle B\rangle$ and $\langle S\rangle$, respectively. The deviation of B and S from their mean value are expressed by $\delta B = B - \langle B\rangle$ and $\delta S = S - \langle S\rangle$, respectively. Thus, according to Eq. (2), the various order mixed cumulants of event-by-event distributions of the two random variables B and S are defined as

$$C(S,S) = C_2^S = \langle(\delta S)^2\rangle, \tag{3}$$

$$C(B,S) = C_{11}^{BS} = \langle\delta B\delta S\rangle, \tag{4}$$

$$C(S,S,S,S) = C_4^S = \langle(\delta S)^4\rangle - 3\langle(\delta S)^2\rangle, \tag{5}$$

$$C(B,S,S,S) = C_{13}^{BS} = \langle\delta B(\delta S)^3\rangle - 3\langle\delta B\delta S\rangle\langle(\delta S)^2\rangle, \tag{6}$$

$$\begin{aligned} C(B,B,S,S) = C_{22}^{BS} &= \langle(\delta B)^2(\delta S)^2\rangle - 2\langle(\delta B\delta S)^2\rangle \\ &\quad - \langle(\delta B)^2\rangle\langle(\delta S)^2\rangle, \end{aligned} \tag{7}$$

$$C(B,B,B,S) = C_{31}^{BS} = \langle(\delta B)^3\delta S\rangle - 3\langle\delta B\delta S\rangle\langle(\delta B)^2\rangle. \tag{8}$$

Once we have the definition of mixed cumulants, the ratio of mixed cumulants can be calculated. A system in thermal equilibrium (for a grand-canonical ensemble) can be characterized by its pressure [22]. The dimensionless pressure of a hadron resonance gas is expressed through the logarithm of the QCD partition function [23],

$$\begin{aligned} \frac{P}{T^4} &= \frac{1}{VT^3}\ln[Z(V,T,\mu_B,\mu_S,\mu_Q)] \\ &= \frac{1}{2\pi}\sum_{i\in X} g_i\left(\frac{m_i}{T}\right)^2 K_2\left(\frac{m_i}{T}\right) \\ &\quad\times\cosh(B_i\hat{\mu}_B + Q_i\hat{\mu}_Q + S_i\hat{\mu}_S), \end{aligned} \tag{9}$$

where g_i is the degeneracy factor for hadrons of mass m_i, and $\hat{\mu}_q \equiv \frac{\mu_q}{T}$, where $q = B_i, S_i$, and Q_i denote the net-baryon number, net strangeness, and the net charge, respectively, and μ_B, μ_S, and μ_Q are the corresponding chemical potentials. For simplicity, we have set the electric charge chemical potential $\hat{\mu}_Q = 0$. These dimensionless fluctuations and correlations of conserved charges (net-baryon number B, net strangeness S) are formally equivalent to the Taylor expansion coefficients of the pressure with the respective chemical potentials [24–26],

$$\chi_{mn}^{BS}(T,\vec{\mu}) = \left.\frac{\partial^{(m+n)}[P(\hat{\mu}_B,\hat{\mu}_S)/T^4]}{\partial\hat{\mu}_B^m\hat{\mu}_S^n}\right|_{\mu_B=\mu_S=0}, \tag{10}$$

where $\hat{\mu}_B = \frac{\mu_B}{T}$ and $\hat{\mu}_S = \frac{\mu_S}{T}$ are the dimensionless baryon and strangeness chemical potentials, $\chi_{0n}^{BS} \equiv \chi_n^S$ and $\chi_{m0}^{BS} \equiv \chi_m^B$. They are also called generalized susceptibilities. All these derivatives are evaluated at $\mu_B = \mu_S = 0$; the expectation values of all net charge numbers vanish (i.e., $\langle B\rangle = \langle S\rangle = 0$) [27]. Theoretically, the mixed cumulants of these conserved quantities are connected to the corresponding susceptibilities by

$$C_{mn}^{BS} = VT^3\chi_{mn}^{BS}(T,\vec{\mu}), \tag{11}$$

where the V and T denote, respectively, the volume and temperature of the system.

If above the transition temperature the quarks can be well described by uncorrelated quasiparticles, then any object that carries strangeness necessarily is a strange quark, which carries a baryon number in proportion to strangeness, $B_s = -\frac{1}{3}S_s$ [28]. Also, from Eq. (10), we can derive

$$\frac{\chi_{mn}^{BS}}{\chi_{m+n}^{S}} = \frac{(-1)^n}{3^m}, \tag{12}$$

where $m,n > 0$ and $m + n = 2,4$. Thus, one expects baryon number and strangeness to be correlated more strongly in a quark-gluon plasma than in a hadron gas. The hot medium created in relativistic heavy-ion collisions is an expanding system; the spatial volume is changing with time evolution. To cancel the effect of the spatial volume dependence to first order, the ratios $\frac{\chi_{11}^{BS}}{\chi_2^S}$, $\frac{\chi_{13}^{BS}}{\chi_4^S}$, $\frac{\chi_{22}^{BS}}{\chi_4^S}$, and $\frac{\chi_{31}^{BS}}{\chi_4^S}$ are constructed. To quantify this and make these ratios to be unity for a system where the relevant degree of freedom is quarks, we introduce

the following normalized ratios in Eqs. (13)–(16):

$$R_{11}^{BS} = -3\frac{C_{11}^{BS}}{C_2^S} = -3\frac{\langle BS\rangle - \langle B\rangle\langle S\rangle}{\langle S^2\rangle - \langle S\rangle^2}, \tag{13}$$

$$R_{13}^{BS} = -3\frac{C_{13}^{BS}}{C_4^S} = -3\frac{\langle BS^3\rangle - 3\langle BS^2\rangle\langle S\rangle - 3\langle BS\rangle(\langle S^2\rangle - 2\langle S\rangle^2) + 6\langle B\rangle\langle S\rangle(\langle S^2\rangle - \langle S\rangle^2) - \langle B\rangle\langle S^3\rangle}{\langle S^4\rangle - 4\langle S^3\rangle\langle S\rangle - 3\langle S^2\rangle^2 + 12\langle S^2\rangle\langle S\rangle^2 - 6\langle S\rangle^4}, \tag{14}$$

$$R_{22}^{BS} = 9\frac{C_{22}^{BS}}{C_4^S} = 9\frac{\langle B^2S^2\rangle - 2\langle B^2S\rangle\langle S\rangle - 2\langle BS\rangle(\langle BS\rangle - 4\langle B\rangle\langle S\rangle) - 2\langle BS^2\rangle\langle B\rangle + 2\langle B\rangle^2(\langle S^2\rangle - 3\langle S\rangle^2) - \langle B^2\rangle\langle S^2\rangle}{\langle S^4\rangle - 4\langle S^3\rangle\langle S\rangle - 3\langle S^2\rangle^2 + 12\langle S^2\rangle\langle S\rangle^2 - 6\langle S\rangle^4}, \tag{15}$$

$$R_{31}^{BS} = -27\frac{C_{31}^{BS}}{C_4^S} = -27\frac{\langle B^3S\rangle - 3\langle B^2S\rangle\langle B\rangle - 3\langle BS\rangle(\langle B^2\rangle - 2\langle B\rangle^2) + 6\langle B\rangle\langle S\rangle(\langle B^2\rangle - \langle B\rangle^2) - \langle B^3\rangle\langle S\rangle}{\langle S^4\rangle - 4\langle S^3\rangle\langle S\rangle - 3\langle S^2\rangle^2 + 12\langle S^2\rangle\langle S\rangle^2 - 6\langle S\rangle^4}. \tag{16}$$

At vanishing chemical potentials, the mean values of the conserved charges are vanishing $\langle B\rangle = \langle S\rangle = 0$, the above equations can be simplified as

$$R_{11}^{BS}\big|_{\mu_B,\mu_S=0} = -3\frac{\langle BS\rangle}{\langle S^2\rangle}, \tag{17}$$

$$R_{13}^{BS}\big|_{\mu_B,\mu_S=0} = -3\frac{\langle BS^3\rangle - 3\langle BS\rangle\langle S^2\rangle}{\langle S^4\rangle - 3\langle S^2\rangle^2}, \tag{18}$$

$$R_{22}^{BS}\big|_{\mu_B,\mu_S=0} = 9\frac{\langle B^2S^2\rangle - 3\langle B^2\rangle\langle S^2\rangle}{\langle S^4\rangle - 3\langle S^2\rangle^2}, \tag{19}$$

$$R_{31}^{BS}\big|_{\mu_B,\mu_S=0} = -27\frac{\langle B^3S\rangle - 3\langle BS\rangle\langle B^2\rangle}{\langle S^4\rangle - 3\langle S^2\rangle^2}. \tag{20}$$

For illustration and discussion purpose, the formulas with $\mu_B = \mu_S = 0$ are just to demonstrate a special case, which is not used in the calculations presented subsequently.

A. Baryon-strangeness correlations in the quark-gluon plasma

At high temperature, the basic degrees of freedom are weakly interacting quarks and gluons. The quark operators u, d, and s represent the net-quark number of up, down, and strange quarks, respectively. We expressed R_{11}^{BS}, R_{13}^{BS}, R_{22}^{BS}, and R_{31}^{BS} in terms of quark degrees of freedom, noting that the baryon number of a quark is $\frac{1}{3}$ and the strangeness of a strange quark is -1 [29]. In terms of quark flavors, the various order ratios R_{11}^{BS}, R_{13}^{BS}, R_{22}^{BS}, R_{31}^{BS} can be written as

$$R_{11}^{BS}\big|_{\mu_B,\mu_S=0} = \frac{\langle (u+d+s)s\rangle}{\langle s^2\rangle} = 1 + \frac{\langle us\rangle + \langle ds\rangle}{\langle s^2\rangle}, \tag{21}$$

$$R_{13}^{BS}\big|_{\mu_B,\mu_S=0} = \frac{\langle (u+d+s)s^3\rangle - 3\langle (u+d+s)s\rangle\langle s^2\rangle}{\langle s^4\rangle - 3\langle s^2\rangle^2} = 1 + \frac{\langle us^3\rangle + \langle ds^3\rangle - 3(\langle us\rangle + \langle ds\rangle)\langle s^2\rangle}{\langle s^4\rangle - 3\langle s^2\rangle^2}, \tag{22}$$

$$\begin{aligned} R_{22}^{BS}\big|_{\mu_B,\mu_S=0} &= \frac{\langle (u+d+s)^2s^2\rangle - 3\langle (u+d+s)^2\rangle\langle s^2\rangle}{\langle s^4\rangle - 3\langle s^2\rangle^2} \\ &= 1 + \frac{\langle (u+d)^2s^2\rangle + 2\langle (u+d)s^3\rangle - 3[\langle (u+d)^2\rangle + 2\langle (u+d)s\rangle]\langle s^2\rangle}{\langle s^4\rangle - 3\langle s^2\rangle^2}, \end{aligned} \tag{23}$$

$$\begin{aligned} R_{31}^{BS}\big|_{\mu_B,\mu_S=0} &= \frac{\langle (u+d+s)^3s\rangle - 3\langle (u+d+s)s\rangle\langle (u+d+s)^2\rangle}{\langle s^4\rangle - 3\langle s^2\rangle^2} \\ &= 1 + \frac{\langle (u+d)^3s\rangle + 3\langle (u+d)^2s^2\rangle - 3\langle (u+d)^2\rangle\langle s^2\rangle + 3\langle (u+d)s^3\rangle}{\langle s^4\rangle - 3\langle s^2\rangle^2} \\ &\quad - \frac{-3\langle (u+d)s\rangle[\langle (u+d)^2\rangle + 2\langle (u+d)s\rangle + 3\langle s^2\rangle]}{\langle s^4\rangle - 3\langle s^2\rangle^2}. \end{aligned} \tag{24}$$

For uncorrelated quark flavors, off-diagonal susceptibilities are vanishing compared to the diagonal susceptibilities [30,31] and susceptibilities inclusive of strangeness are smaller than those which involve lighter flavors [32–34]; then we have

$$\langle us\rangle = \langle ds\rangle = 0, \tag{25}$$

$$\chi_{us} = \chi_{ds} \leqslant \chi_{ud} \ll \chi_s \leqslant \chi_d = \chi_u, \tag{26}$$

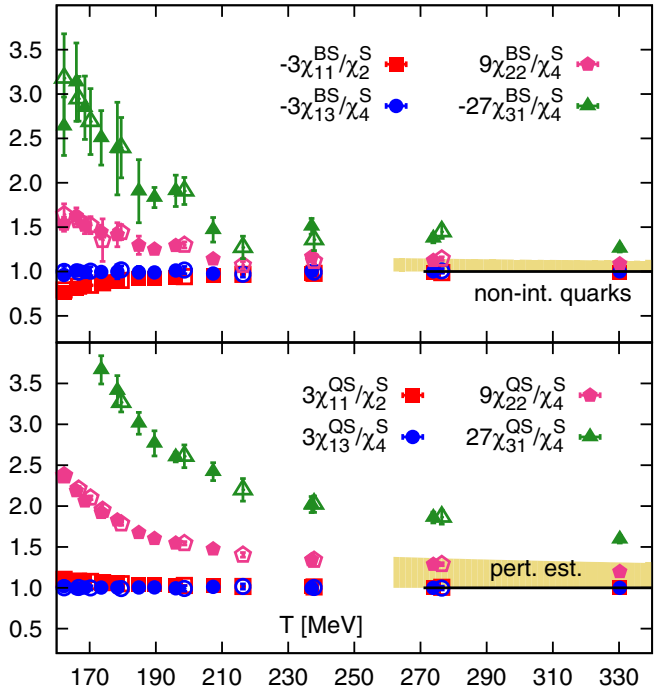

FIG. 1. Baryon-strangeness (top) and electric charge-strangeness correlation (bottom), properly scaled by the strangeness fluctuations and the power of the fractional baryonic and electric charges [see Eq. (12)]. The figure is from Ref. [21].

and thus

$$R^{BS}_{mn}\big|_{\mu_B,\mu_S=0} = 1, \tag{27}$$

where $m,n > 0$ and $m + n = 2, 4$.

In the noninteracting massless quark gas all these observables are unity (shown by the lines at high temperatures in Fig. 1). At high temperatures, the shaded regions indicate the ranges of values for these ratios, as predicted for the weakly interacting quasiquarks from the resummed hard thermal loop (HTL) perturbation theory at the one-loop order [35,36].

B. Baryon-strangeness correlations in free hadron resonance gas

It is well known that at low temperature and chemical potentials the QCD can be modeled as a gas of uncorrelated hadrons, where interactions are included through resonances [37]. These states are taken from Particle Data Book [38]. As the interactions between hadrons are suppressed, the contributions of individual hadrons to thermodynamics can be regarded as free Boltzmann gas [3]. For a gas of uncorrelated hadron resonances, from Eqs. (13)–(16), the numerator receives contributions from only (strange) baryons and antibaryons, while the denominator receives contributions also from strange mesons [37,39]. Equation (13) can be written as

$$R^{BS}_{11} \approx 3\frac{\langle\Lambda\rangle + \langle\bar{\Lambda}\rangle + \cdots + 3\langle\Omega^-\rangle + 3\langle\bar{\Omega}^+\rangle}{\langle K^0\rangle + \langle\bar{K}^0\rangle + \cdots + 9\langle\Omega^-\rangle + 9\langle\bar{\Omega}^+\rangle}. \tag{28}$$

Reference [21] gives the lattice QCD results for the appropriate combinations of up to fourth-order cumulants of net-strangeness fluctuations and their correlations with net-baryon number and electric charge fluctuations, shown in Fig. 1. The ratios of the second-order correlations $\chi^{BS}_{11}/\chi^{S}_{2}$ and $\chi^{QS}_{11}/\chi^{S}_{2}$ are much closer to the expectations for weakly interacting quasiquarks, differing only around T–$1.25T_c$, while the HTL perturbative expansion for ratios involving one derivate of the baryonic/electric charges ($\chi^{XS}_{11}/\chi^{S}_{2}$ and $\chi^{XS}_{13}/\chi^{S}_{4}$) [40] starts differing from the noninteracting quark gas limit [21]. It is the same for those involving higher derivatives of the baryonic/electric charges ($\chi^{XS}_{22}/\chi^{4}_{2}$ and $\chi^{XS}_{31}/\chi^{S}_{4}$).

IV. RESULTS

In this paper, we performed our calculations with the UrQMD model in version 2.3 for Au + Au collisions at $\sqrt{s_{NN}} = 7.7, 11.5, 19.6, 27, 39, 62.4, 200$ GeV and the corresponding event statistics are 35×10^6, 105×10^6, 106×10^6, 81×10^6, 133×10^6, 38×10^6, and 56×10^6, respectively [41]. The statistical errors are calculated by the formulas that are derived from the standard error propagations (see the Appendix). To avoid autocorrelations, we define the centralities with the charged particles within the pseudorapidity $0.5 < |\eta| < 1$ and perform the analysis in the pseudorapidity range ($|\eta| < 0.5$). For the B-S correlations, we include the particles p, n, K^+, K^0, Λ, Σ^-, Σ^0, Σ^+, Ξ^-, Ξ^0, and Ω^- and their antiparticles. These particles can be classified into strange baryons (Λ, Σ, Ξ, Ω), nonstrange baryons (p,n), and strange mesons (K,K^0). To study the contributions of various hadron species to the baryon-strangeness correlations, we consider the B-S correlations with the following combinations of hadrons:

(i) net p vs net K, only p, $\bar{p}$, K^+, K^- are included;
(ii) net p vs net Λ, only p, $\bar{p}$, Λ, $\bar{\Lambda}$ are included;
(iii) net Λ vs net K, only Λ, $\bar{\Lambda}$, K^+, K^- are included;
(iv) B-S (all particles): p, n, K^+, K^0, Λ, Σ, Ξ, Ω and their antiparticles are included;
(v) B-S (excluding strange baryon), only p, n, K^+, K^0 are included;
(vi) B-S (excluding Λ, $\bar{\Lambda}$), only p, n, K^+, K^0, Σ, Ξ, Ω and their antiparticles are included;
(vii) B-S (excluding nonstrange baryon), only K^+, K^0, Λ, Σ, Ξ, Ω and their antiparticles are included;
(viii) B-S (excluding p, $\bar{p}$), only n, K^+, K^0, Λ, Σ, Ξ, Ω and their antiparticles are included;
(ix) B-S (excluding strange meson), only p, n, Λ, Σ, Ξ, Ω and their antiparticles are included;
(x) B-S (excluding K^+, K^-), only p, n, K^0, Λ, Σ, Ξ, Ω and their antiparticles are included.

Figure 2 shows the centrality dependence for cases (iv)–(x) in the Au + Au collisions at $\sqrt{s_{NN}} = 39$ GeV from the UrQMD model. The top panels of Fig. 2 display the two-dimensional correlations for cases (iv)–(x) for the most central (0%–5%) Au + Au collisions. To quantify the correlation strength, we calculated the standard correlation coefficient for each case. In statistics, the correlation coefficient (ρ) is a measure of the linear dependence between two variables X and Y, and it is the covariance of the two variables divided by

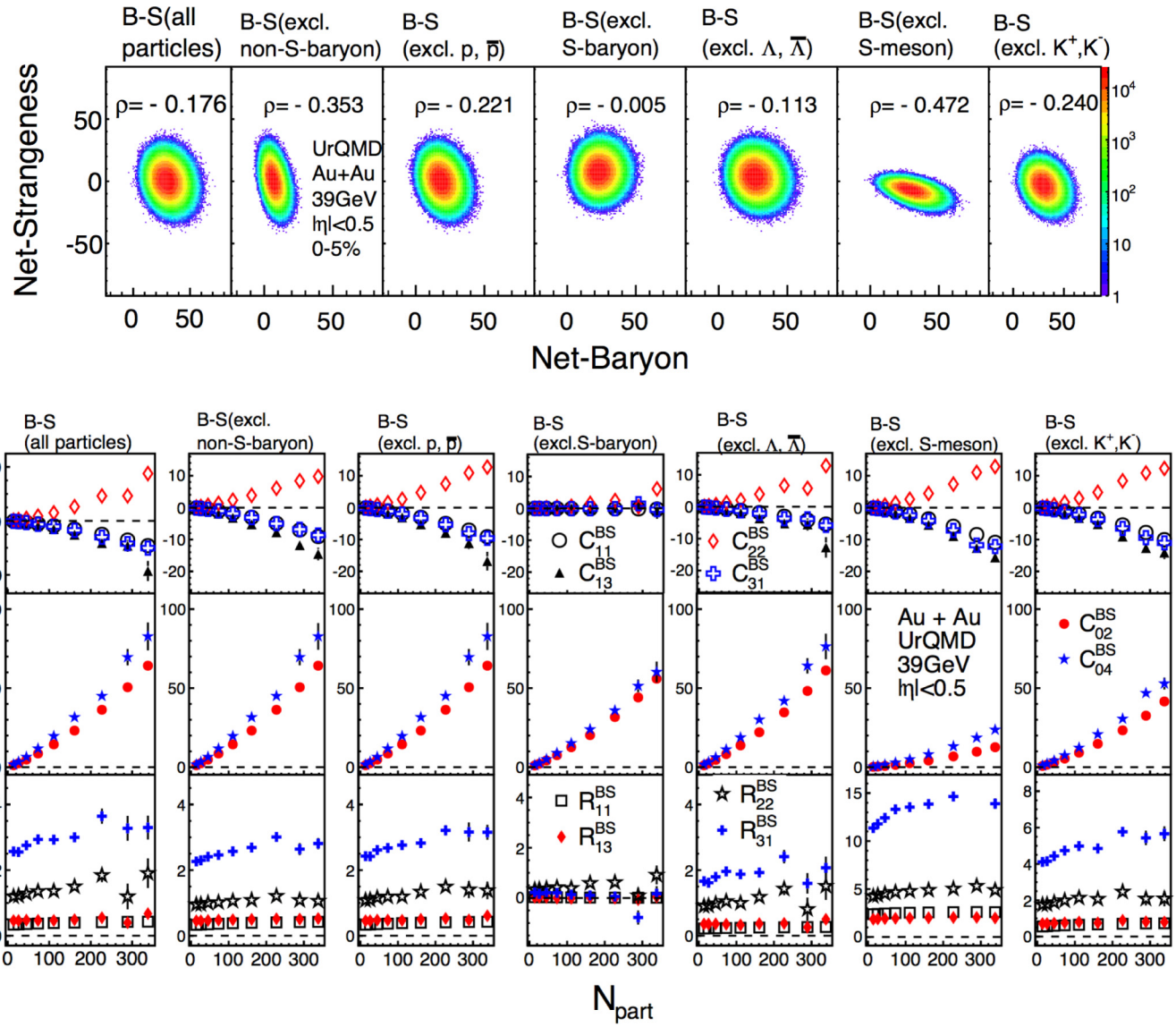

FIG. 2. (Top) The baryon-strangeness correlations for cases (iv)–(x) in the most central (0%–5%) Au + Au collisions at $\sqrt{s_{NN}} = 39$ GeV from the UrQMD model. (Bottom) The centrality dependence of various order mixed cumulants (C_{11}^{BS}, C_{13}^{BS}, C_{22}^{BS}, C_{31}^{BS}, C_{02}^{BS}, C_{04}^{BS}) and ratios (R_{11}^{BS}, R_{13}^{BS}, R_{22}^{BS}, R_{31}^{BS}) of (iv)–(x) at $\sqrt{s_{NN}} = 39$ GeV for Au + Au collisions from the UrQMD model.

the product of their standard deviations. It is defined as

$$\rho_{X,Y} = \frac{\mathrm{cov}(X,Y)}{\sigma_X \sigma_Y} = \frac{\langle (X - \langle X \rangle)(Y - \langle Y \rangle) \rangle}{\sqrt{\langle X^2 \rangle - \langle X \rangle^2}\sqrt{\langle Y^2 \rangle - \langle Y \rangle^2}},$$

where $\mathrm{cov}(X,Y)$ is the covariance between random variables X and Y. σ_X and σ_Y are the standard deviations of X and Y, respectively. The definition gives a value between $+1$ and -1, where a value of 1 represents strong correlation, a value of 0 indicates no linear correlation, and a value of -1 gives perfect anticorrelation. These two-dimensional plots indicate that most of the cases are anticorrelated and dominated by the strange baryons, such as Λ. The bottom panels of Fig. 2 show the centrality dependence of mixed cumulants (C_{11}^{BS}, C_{13}^{BS}, C_{22}^{BS}, C_{31}^{BS}, C_{02}^{BS}, C_{04}^{BS}) and ratios (R_{11}^{BS}, R_{13}^{BS}, R_{22}^{BS}, R_{31}^{BS}) for cases (iv)–(x) in Au + Au collisions at $\sqrt{s_{NN}} = 39$ GeV. It is found that the C_{11}^{BS}, C_{13}^{BS}, and C_{31}^{BS} have negative values, while C_{22}^{BS} have positive values. A strong centrality dependence for the baryon-strangeness (B-S) correlations for cases (vi)–(x) is observed. By comparing case (iv) with case (v), we find that the strange baryons have significant contributions to the baryon-strangeness correlations, and the strange mesons ($K^{\pm}$ and K^0) contribute significantly to strangeness fluctuations of case (ix) [42]. When the strange baryons are excluded from the B-S correlations, the mixed-cumulant ratios are much smaller than the case with all particles and have values close to zero. However, when the strange mesons are excluded from the B-S correlations, the values of the ratios (R_{11}^{BS}, R_{13}^{BS}, R_{22}^{BS}, R_{31}^{BS}) become larger than those in the case with all particles. Furthermore, the results from the case where the nonstrange baryons are not included is very close to the results from the case with all particles included. This indicates that the nonstrange baryons have little contribution to the

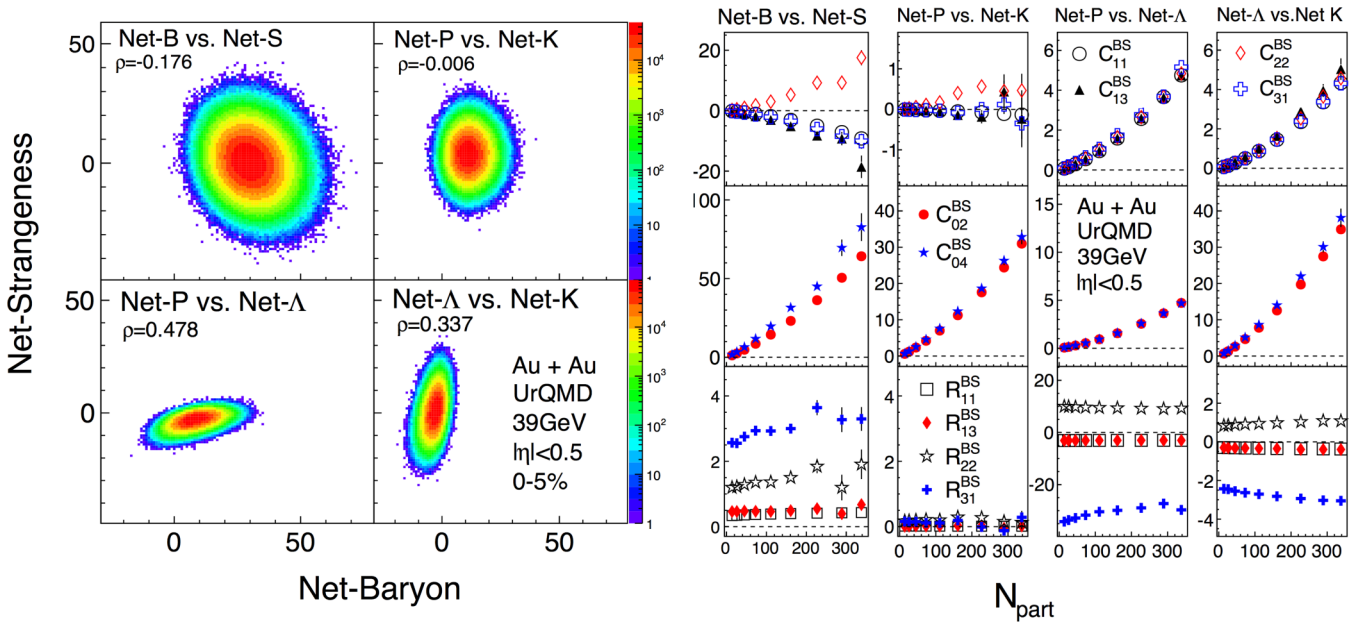

FIG. 3. (Left) The correlation between net baryon and net strangeness of (i)–(iv) at $\sqrt{s_{NN}} = 39$ GeV for the most central (0%–5%) Au + Au collision from the UrQMD model. (Right) The centrality dependence of mixed cumulants (C_{11}^{BS}, C_{13}^{BS}, C_{22}^{BS}, C_{31}^{BS}, C_{02}^{BS}, C_{04}^{BS}) and ratios (R_{11}^{BS}, R_{13}^{BS}, R_{22}^{BS}, R_{31}^{BS}) for (i)–(iv) at $\sqrt{s_{NN}} = 39$ GeV for Au + Au collisions from the UrQMD model.

baryon-strangeness correlations. Because these ratios show weak centrality dependence, we will only consider the most central (0%–5%) collision centralities for the energy dependence.

Figure 3 shows the centrality dependence of B-S correlations for cases (i)–(iv) in Au + Au collisions at $\sqrt{s_{NN}} =$ 39 GeV. The left panels of Fig. 3 show the correlations for different cases in the most central (0%–5%) Au + Au collisions. The right panels of Fig. 3 show the centrality dependence of mixed cumulants (C_{11}^{BS}, C_{13}^{BS}, C_{22}^{BS}, C_{31}^{BS}, C_{02}^{BS}, C_{04}^{BS}) and ratios (R_{11}^{BS}, R_{13}^{BS}, R_{22}^{BS}, R_{31}^{BS}) for cases (i)–(iv). In the two-dimensional plots, we find that the net baryon versus net strangeness shows strong anticorrelations. If the strange baryons are excluded, for example, the net-proton and net-kaon correlations are almost independent of each other ($\rho \sim 0$). It indicates that the strange baryons play an important role and have significant contributions to the B-S correlations. In the B-S correlations with all particles, the C_{11}^{BS}, C_{13}^{BS}, and C_{31}^{BS} show negative values and monotonically decrease with increasing of the number of participant nucleons in the collisions, while the C_{22}^{BS} have large and positive values for all of the cases. Interestingly, the ratios R_{11}^{BS}, R_{13}^{BS}, R_{22}^{BS}, and R_{31}^{BS} with all particles included show weak centrality dependence and are comparable with the lattice QCD results shown in Fig. 1. In the left panels of Fig. 3, the net proton and net Λ, net K, and net Λ show finite positive correlations. This can be understood in terms of the baryon stopping and associated productions of the K^+ and Λ. Their mixed cumulants are positive values, but the ratios R_{11}^{BS}, R_{13}^{BS}, and R_{31}^{BS} are negative. Furthermore, the variance of the fluctuation of net Λ is much smaller than the variance of net-kaon distributions. This leads to bigger deviation from zero for the proton-Λ than kaon-Λ correlations.

Figure 4 shows the energy dependence of the mixed cumulants and ratios for cases (i)–(iv) in the most central (0%–5%) Au + Au collisions from the UrQMD model. In the B-S correlation including all particles, the mixed cumulants C_{11}^{BS}, C_{13}^{BS}, and C_{31}^{BS} are negative and show weak energy dependence, while C_{02}^{BS}, C_{04}^{BS}, and C_{22}^{BS} are positive and monotonically increase with increasing energy. However, the ratios R_{11}^{BS}, R_{13}^{BS}, R_{22}^{BS} show weak energy dependence, but the ratio R_{31}^{BS} decreases at low energies. This decreasing trend of the R_{31}^{BS} is also observed in the correlations between net proton

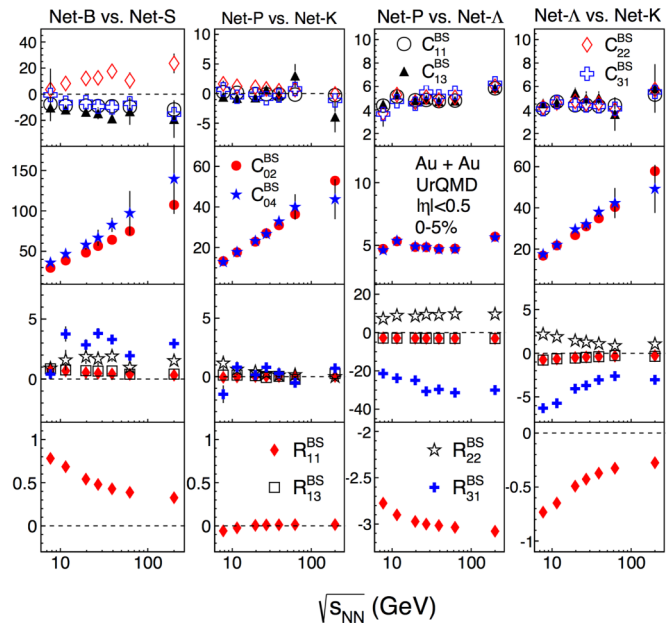

FIG. 4. The energy dependence of mixed cumulants and ratios of cases (i)–(iv) for the most central (0%–5%) Au + Au collisions from the UrQMD model.

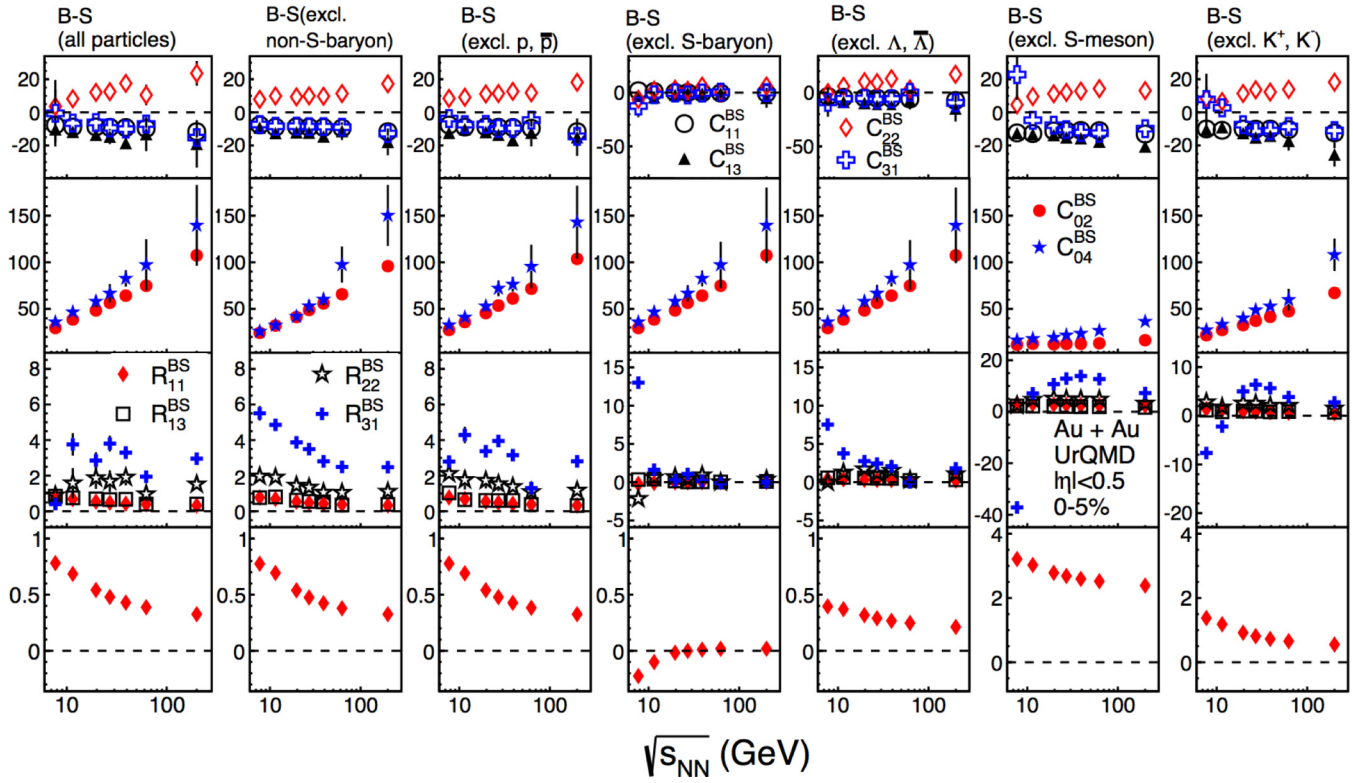

FIG. 5. The energy dependence of various order mixed cumulants (C_{11}^{BS}, C_{13}^{BS}, C_{22}^{BS}, C_{31}^{BS}, C_{02}^{BS}, C_{04}^{BS}) and ratios (R_{11}^{BS}, R_{13}^{BS}, R_{22}^{BS}, R_{31}^{BS}) of cases (iv)–(x) at $\sqrt{s_{NN}} = 7.7$, 11.5, 19.6, 27, 39, 62.4, and 200 GeV for the most central (0%–5%) Au + Au collision from the UrQMD model.

and net kaon, which might originate from the associated production of K^+ by the reaction channel $NN \rightarrow NYK$, where N stands for nucleon and Y stands for hyperon. The trends of these ratios for the correlations between net proton and net Λ are opposite to the trends observed in the net-kaon and net-Λ correlations. For these two cases, the mixed-cumulant ratios R_{11}^{BS}, R_{13}^{BS}, and R_{31}^{BS} are negative, R_{22}^{BS} is positive, but higher-order ratios R_{22}^{BS} and R_{31}^{BS} have larger value. To demonstrate the energy dependence of the second-order ratio R_{11}^{BS} more clearly, we plot R_{11}^{BS} as a function of energy in the bottom panels of Fig. 4. It is found that when all particles are considered or only proton and λ are included, the R_{11}^{BS} decreases with increasing energy, while we observe different trends for the other two cases. At low energy, the higher-order ratio R_{31}^{BS} becomes small for cases (i) (net p vs net K) and (iv) (net B vs net S), the main reason is probably because at low energy, the baryon stopping of protons and associated kaon production play important roles.

Figure 5 shows the energy dependence of various order mixed cumulants and ratios of the baryon-strangeness correlations for cases (iv)–(x) for the most central (0%–5%) Au + Au collisions from the UrQMD model. By excluding the nonstrange baryons from the B-S correlations, we find that the values of ratios R_{11}^{BS}, R_{13}^{BS}, R_{22}^{BS}, R_{31}^{BS} are finite and monotonically increase with decreasing collision energy; it is comparable with the results from lattice QCD at low temperature (lattice QCD results shown in Fig. 1). For the R_{11}^{BS}, the case including all particles is very close to the one excluding nonstrange baryons or protons, while they are different for R_{31}^{BS}. It means the nonstrange baryons have small effects on the second-order ratio R_{11}^{BS}, while they have large effects on the higher-order ratio. However, if we exclude the strange baryons or Λ, the values of baryon-strangeness correlations are close to zero at high energies. It indicates that the strange baryons, especially the Λ baryons, carry significant information and play an important role for the B-S correlations. Especially, the R_{31}^{BS} show large increase at low energy. It is probably because Λ is the lightest strange baryon and contributes most significantly to the baryon-strangeness correlations. When the K^+ and K^- are excluded, there are large impacts on the higher-order ratio R_{31}^{BS} at low energies. The ratio becomes negative, which is probably attributable to the kaon associated production at low energy. There is a strong correlation between protons and kaons, as shown in the Fig. 4. If we remove the kaons from the B-S correlations, the correlations between proton and Λ will dominate the B-S correlations, which is negative.

V. SUMMARY

We have analyzed the centrality and energy dependence of the baryon-strangeness (B-S) correlations in Au + Au collisions at $\sqrt{s_{NN}} = 7.7$, 11.5, 19.6, 27, 39, 62.4, and 200 GeV from the UrQMD model. The B-S correlations are studied via various order mixed cumulants and corresponding ratios. The B-S correlations are studied via various order mixed cumulants and corresponding ratios. Such a study provides the following important features. (1) It provides an expectation from a non-CP-based model on B-S correlations. The model incorporates standard physics related to baryon

number, strangeness number, and charge conservation. It also models the baryon stopping at lower beam energies. In addition, it incorporates resonances, their decay and particle interactions in a hadronic matter. (2) The UrQMD model in this paper is treated as datalike, and we have discussed the ways to construct feasible B-S correlations which can be experimentally measured. (3) The B-S correlations results presented in this paper from the analysis of the UrQMD model data as one would have carried out in a manner as one would do it using the real experimental data. It has been done using typical acceptance cuts, avoiding autocorrelations while choosing the particle multiplicity used to define the collision centrality and to calculate the correlations, derive the expressions for the statistical errors for such correlations, etc. Our results presented in this paper provide a methodology to look at the experimental data.

We have presented the B-S correlations by excluding different hadron species, we have studied ten different cases: (i)–(x). In these studies, we observed strong correlations between net proton and net Λ at low energies, which could be related to the baryon stopping and associated production of the hyperons and kaons. The various results of the mixed cumulants and ratios obtained from UrQMD calculations show a weak centrality dependence. As far as the energy dependence is concerned, we observe that the strange baryons and strange mesons have significant contributions to baryon-strangeness correlations and various order mixed-cumulant ratios R_{13}^{BS}, R_{13}^{BS}, R_{22}^{BS}, and R_{31}^{BS}, especially at low energy. When strange baryons are excluded from the B-S correlations, the values are relatively small and close to zero. It is found that the model results are also comparable with the lattice QCD calculations at low temperature.

Thus, our studies presented in this paper have provided the expectations on the interplay of baryon stopping and kaon associated production to B-S correlations at different collision energies from the UrQMD model. They also provide a baseline for the B-S correlations as an observable to search for the signals of the QCD phase transition and critical point in heavy-ion collisions.

ACKNOWLEDGMENTS

The work was supported in part by the MoST of China 973-Project No. 2015CB856901, NSFC under Grant No. 11575069. B.M. is supported by DAE, DST, and SERB, Government of India.

APPENDIX: STATISTICAL ERROR CALCULATIONS

It is well known that the variance of statistic $\Phi(X_1, X_1, \ldots, X_m)$ can be expressed in terms of the following [43]:

$$V(\Phi) = \sum_{i=1,j=1}^{m} \left(\frac{\partial \Phi}{\partial X_i}\right)\left(\frac{\partial \Phi}{\partial X_j}\right)\mathrm{cov}(X_i, X_j). \tag{A1}$$

The covariance of the multivariate moments can be written as [44]

$$\mathrm{cov}(f_{i,j}, f_{k,h}) = \frac{1}{N}(f_{i+k,j+h} - f_{i,j} f_{k,h}), \tag{A2}$$

where N is the number of events, $f_{i,j} = \langle B^i S^j \rangle$ and $f_{k,h} = \langle B^k S^h \rangle$ are the joint moments of net baryon and net strangeness.

We use $F_{m,n}$ to present the mixed-central moments,

$$\begin{aligned} F_{m,n} &= \langle (\delta B)^m (\delta S)^n \rangle \\ &= \sum_{i=0}^{m}\sum_{j=0}^{n} C_m^i C_n^j (-1)^{m+n-i-j} f_{1,0}^{m-i} f_{0,1}^{n-j} f_{i,j}. \end{aligned} \tag{A3}$$

The partial derivation of $F_{m,n}$ to its variable $f_{i,j}$ is

$$D_{m,n,i,j} = \frac{\partial F_{m,n}}{\partial f_{i,j}} = \sum_{i=0}^{m}\sum_{j=0}^{n} C_m^i C_n^j (-1)^{m+n-i-j} f_{1,0}^{m-i} f_{0,1}^{n-j}. \tag{A4}$$

The various order mixed-cumulant ratios can be expressed by the terms of joint moments:

$$R_{11}^{BS} = -3\frac{C_{11}^{BS}}{C_{02}^{BS}} = -3\frac{F_{1,1}}{F_{0,2}} = -3\frac{f_{1,1} - f_{0,1} f_{1,0}}{f_{0,2} - f_{0,1}^2}, \tag{A5}$$

$$\begin{aligned} R_{13}^{BS} &= -3\frac{C_{13}^{BS}}{C_{04}^{BS}} = -3\frac{F_{1,3} - 3F_{1,1}F_{0,2}}{F_{0,4} - 3F_{0,2}^2} \\ &= -3\frac{f_{1,3} - 3f_{1,2}f_{0,1} + 6f_{1,1}f_{0,1}^2 + 6f_{1,0}f_{0,2}f_{0,1} - 3f_{1,1}f_{0,2} - 6f_{1,0}f_{0,1}^3 - f_{1,0}f_{0,3}}{f_{0,4} - 4f_{0,3}f_{0,1} - 3f_{0,2}^2 + 12f_{0,2}f_{0,1}^2 - 6f_{0,1}^4}, \end{aligned} \tag{A6}$$

$$\begin{aligned} R_{22}^{BS} &= 9\frac{C_{22}^{BS}}{C_{04}^{BS}} = 9\frac{F_{2,2} - 2F_{1,1}^2 - F_{0,2}F_{2,0}}{F_{0,4} - 3F_{0,2}^2} \\ &= 9\frac{-6f_{0,1}^2 f_{1,0}^2 + 2f_{0,2}f_{1,0}^2 + 8f_{0,1}f_{1,0}f_{1,1} - 2f_{1,1}^2 - 2f_{1,0}f_{1,2} + 2f_{2,0}f_{0,1}^2 - f_{2,0}f_{0,2} - 2f_{0,1}f_{2,1} + f_{2,2}}{f_{0,4} - 4f_{0,3}f_{0,1} - 3f_{0,2}^2 + 12f_{0,2}f_{0,1}^2 - 6f_{0,1}^4}, \end{aligned} \tag{A7}$$

$$\begin{aligned} R_{31}^{BS} &= -27\frac{C_{31}^{BS}}{C_{04}^{BS}} = -27\frac{F_{3,1} - 3F_{1,1}F_{2,0}}{F_{0,4} - 3F_{0,2}^2} \\ &= -27\frac{f_{3,1} - 3f_{2,1}f_{1,0} + 6f_{1,1}f_{1,0}^2 + 6f_{1,0}f_{2,0}f_{0,1} - 3f_{1,1}f_{2,0} - 6f_{0,1}f_{1,0}^3 - f_{0,1}f_{3,0}}{f_{0,4} - 4f_{0,3}f_{0,1} - 3f_{02}^2 + 12f_{0,2}f_{0,1}^2 - 6f_{0,1}^4}. \end{aligned} \tag{A8}$$

The partial derivation of R_{11}^{BS} to its variable $f_{i,j}$ is

$$\frac{\partial R_{11}^{BS}}{\partial f_{ij}} = \frac{\partial R_{11}^{BS}}{\partial F_{1,1}}\frac{\partial F_{1,1}}{\partial f_{i,j}} + \frac{\partial R_{11}^{BS}}{\partial F_{0,2}}\frac{\partial F_{0,2}}{\partial f_{i,j}} = \frac{-3}{C_{02}^{BS}}D_{1,1,i,j} + \frac{3C_{11}^{BS}}{\left(C_{02}^{BS}\right)^2}D_{0,2,i,j}. \tag{A9}$$

The variance of observable R_{11}^{BS} is

$$V\left(R_{11}^{BS}\right) = \sum_{i,k=0}^{1}\sum_{j,h=0}^{2}\frac{\partial R_{11}^{BS}}{\partial f_{i,j}}\frac{\partial R_{11}^{BS}}{\partial f_{k,h}}\mathrm{cov}(f_{i,j}, f_{k,h}). \tag{A10}$$

The error of observable R_{11}^{BS} is

$$\mathrm{error}\left(R_{11}^{BS}\right) = \sqrt{V\left(R_{11}^{BS}\right)}. \tag{A11}$$

The partial derivation of R_{13}^{BS} to its variable $f_{i,j}$ is

$$\begin{aligned}\frac{\partial R_{13}^{BS}}{\partial f_{i,j}} &= \frac{\partial R_{13}^{BS}}{\partial F_{1,3}}\frac{\partial F_{1,3}}{\partial f_{i,j}} + \frac{\partial R_{11}^{BS}}{\partial F_{1,1}}\frac{\partial F_{1,1}}{\partial f_{i,j}} + \frac{\partial R_{11}^{BS}}{\partial F_{0,4}}\frac{\partial F_{0,4}}{\partial f_{i,j}} + \frac{\partial R_{11}^{BS}}{\partial F_{0,2}}\frac{\partial F_{0,2}}{\partial f_{i,j}} \\ &= \frac{-3}{C_{04}^{BS}}D_{1,3,i,j} + \frac{3C_{02}^{BS}}{C_{04}^{BS}}D_{1,1,i,j} + \frac{3C_{13}^{BS}}{\left(C_{04}^{BS}\right)^2}D_{0,4,i,j} + \frac{9C_{11}^{BS}C_{04}^{BS} + 18C_{13}^{BS}C_{02}^{BS}}{\left(C_{04}^{BS}\right)^2}D_{0,2,i,j}.\end{aligned} \tag{A12}$$

The variance of observable R_{13}^{BS} is

$$V\left(R_{13}^{BS}\right) = \sum_{i,k=0}^{1}\sum_{j,h=0}^{4}\frac{\partial R_{13}^{BS}}{\partial f_{i,j}}\frac{\partial R_{13}^{BS}}{\partial f_{k,h}}\mathrm{cov}(f_{i,j}, f_{k,h}). \tag{A13}$$

The error of observable R_{13}^{BS} is

$$\mathrm{error}\left(R_{13}^{BS}\right) = \sqrt{V\left(R_{13}^{BS}\right)}. \tag{A14}$$

The partial derivation of R_{22}^{BS} to its variable $f_{i,j}$ is

$$\begin{aligned}\frac{\partial R_{22}^{BS}}{\partial f_{i,j}} &= \frac{\partial R_{22}^{BS}}{\partial F_{2,2}}\frac{\partial F_{2,2}}{\partial f_{i,j}} + \frac{\partial R_{22}^{BS}}{\partial F_{2,0}}\frac{\partial F_{2,0}}{\partial f_{i,j}} + \frac{\partial R_{22}^{BS}}{\partial F_{1,1}}\frac{\partial F_{1,1}}{\partial f_{i,j}} + \frac{\partial R_{22}^{BS}}{\partial F_{0,4}}\frac{\partial F_{0,4}}{\partial f_{i,j}} + \frac{\partial R_{22}^{BS}}{\partial F_{0,2}}\frac{\partial F_{0,2}}{\partial f_{i,j}} \\ &= \frac{9}{C_{04}^{BS}}D_{2,2,i,j} + \frac{-9C_{02}^{BS}}{C_{04}^{BS}}D_{2,0,i,j} + \frac{-36C_{11}^{BS}}{C_{04}^{BS}}D_{1,1,i,j} + \frac{-9C_{22}^{BS}}{\left(C_{04}^{BS}\right)^2}D_{0,4,i,j} + \frac{9C_{20}^{BS}C_{04}^{BS} + 54C_{02}^{BS}C_{22}^{BS}}{\left(C_{04}^{BS}\right)^2}D_{0,2,i,j}.\end{aligned} \tag{A15}$$

The variance of observable R_{22}^{BS} is

$$V\left(R_{22}^{BS}\right) = \sum_{i,k=0}^{2}\sum_{j,h=0}^{4}\frac{\partial R_{22}^{BS}}{\partial f_{i,j}}\frac{\partial R_{22}^{BS}}{\partial f_{k,h}}\mathrm{cov}(f_{i,j}, f_{k,h}). \tag{A16}$$

The error of observable R_{22}^{BS} is

$$\mathrm{error}\left(R_{22}^{BS}\right) = \sqrt{V\left(R_{22}^{BS}\right)}. \tag{A17}$$

The partial derivation of R_{31}^{BS} to its variable $f_{i,j}$ is

$$\begin{aligned}\frac{\partial R_{31}^{BS}}{\partial f_{i,j}} &= \frac{\partial R_{31}^{BS}}{\partial F_{3,1}}\frac{\partial F_{3,1}}{\partial f_{i,j}} + \frac{\partial R_{31}^{BS}}{\partial F_{2,0}}\frac{\partial F_{2,0}}{\partial f_{i,j}} + \frac{\partial R_{31}^{BS}}{\partial F_{1,1}}\frac{\partial F_{1,1}}{\partial f_{i,j}} + \frac{\partial R_{31}^{BS}}{\partial F_{0,4}}\frac{\partial F_{0,4}}{\partial f_{i,j}} + \frac{\partial R_{31}^{BS}}{\partial F_{0,2}}\frac{\partial F_{0,2}}{\partial f_{i,j}} \\ &= \frac{-27}{C_{04}^{BS}}D_{3,1,i,j} + \frac{81C_{11}^{BS}}{C_{04}^{BS}}D_{2,0,i,j} + \frac{81C_{20}^{BS}}{\left(C_{04}^{BS}\right)^2}D_{1,1,i,j} + \frac{27C_{31}^{BS}}{\left(C_{04}^{BS}\right)^2}D_{0,4,i,j} + \frac{-162C_{02}^{BS}C_{31}^{BS}}{\left(C_{04}^{BS}\right)^2}D_{0,2,i,j}.\end{aligned} \tag{A18}$$

The variance of observable R_{31}^{BS} is

$$V\left(R_{31}^{BS}\right) = \sum_{i,k=0}^{3}\sum_{j,h=0}^{4}\frac{\partial R_{31}^{BS}}{\partial f_{i,j}}\frac{\partial R_{31}^{BS}}{\partial f_{k,h}}\mathrm{cov}(f_{i,j}, f_{k,h}). \tag{A19}$$

The error of observable R_{31}^{BS} is

$$\text{error}\left(R_{31}^{BS}\right) = \sqrt{V\left(R_{31}^{BS}\right)}. \tag{A20}$$

[1] M. A. Stephanov, K. Rajagopal, and E. Shuryak, Phys. Rev. Lett. **81**, 4816 (1998); Phys. Rev. D **60**, 114028 (1999); M. A. Stephanov, Phys. Rev. Lett. **102**, 032301 (2009); **107**, 052301 (2011).

[2] S. Jeon and V. Koch, Phys. Rev. Lett. **83**, 5435 (1999); **85**, 2076 (2000).

[3] M. Asakawa, U. Heinz, and B. Muller, Phys. Rev. Lett. **85**, 2072 (2000); M. Asakawa, S. Ejiri, and M. Kitazawa, *ibid.* **103**, 262301 (2009); M. Asakawa and M. Kitazawa, Prog. Part. Nucl. Phys. **90**, 299 (2016).

[4] S. Gupta, X. Luo, B. Mohanty, H. G. Ritter, and N. Xu, Science **332**, 1525 (2012).

[5] S. Borsanyi, PoS (LATTICE 2015) 015; M. Cheng *et al.*, Phys. Rev. D **79**, 074505 (2009).

[6] S. Borsanyi, Z. Fodor, S. D. Katz, S. Krieg, C. Ratti, and K. Szabo, J. High Energy Phys. 01 (2012) 138.

[7] A. Bazavov, H. T. Ding, P. Hegde *et al.*, Phys. Rev. D **88**, 094021 (2013).

[8] R. V. Gavai and S. Gupta, Phys. Rev. D **73**, 014004 (2006); **78**, 114503 (2008).

[9] A. Bazavov, H. T. Ding, P. Hegde *et al.*, Phys. Rev. Lett. **109**, 192302 (2012).

[10] M. M. Aggarwal *et al.*, arXiv:1007.2613.

[11] X. Luo (for the STAR Collaboration), PoS (CPOD2014) 019 [arXiv:1503.02558].

[12] X. Luo, Nucl. Phys. A **956**, 75 (2016).

[13] M. M. Aggarwal *et al.* (STAR Collaboration), Phys. Rev. Lett. **105**, 022302 (2010); L. Adamczyk *et al.* (STAR Collaboration), *ibid.* **113**, 092301 (2014); **112**, 032302 (2014).

[14] H. T. Ding, S. Mukherjee, H. Ohno, P. Petreczky, and H. P. Schadler, Phys. Rev. D **92**, 074043 (2015).

[15] M. Bleicher, S. Jeon, and V. Koch, Phys. Rev. C **62**, 061902(R) (2000).

[16] S. Haussler, H. Stocker, and M. Bleicher, Phys. Rev. C **73**, 021901(R) (2006).

[17] M. Bleicher *et al.*, Phys. G: Nucl. Part. Phys. **25**, 1859 (1999).

[18] S. A. Bass *et al.*, Prog. Part. Nucl. Phys. **41**, 255 (1998).

[19] H. Petersen, M. Bleicher, S. A. Bass, and H. Stocker, arXiv:0805.0567v1 [hep-ph].

[20] C. Ahlbach, J. Usatine, and N. Pippenger, arXiv:1211.0652 [math.CO].

[21] A. Bazavov *et al.*, Phys. Rev. Lett. **111**, 082301 (2013).

[22] A. Bazavov, H.-T. Ding, P. Hegde *et al.*, Phys. Rev. Lett. **113**, 072001 (2014).

[23] P. Alba *et al.*, Phys. Lett. B **738**, 305 (2014).

[24] R. Bellwied, S. Borsanyi, Z. Fodor, S. D. Katz, and C. Ratti, Phys. Rev. Lett. **111**, 202302 (2013).

[25] D. K. Mishra, P. K. Netrakanti, and B. Mohanty, Phys. Rev. C **94**, 054906 (2016).

[26] S. Mukherjee, arXiv:1307.6255.

[27] A. Bazavov *et al.* (HotQCD Collaboration), Phys. Rev. D **86**, 034509 (2012).

[28] V. Koch, arXiv:0810.2520.

[29] P. B. Munzinger *et al.*, Phys. Rep. **621**, 76 (2016).

[30] C. R. Allton, M. Doring, S. Ejiri, S. J. Hands *et al.*, Phys. Rev. D **71**, 054508 (2005).

[31] R. V. Gavai and S. Gupta, Phys. Rev. D **65**, 094515 (2002).

[32] A. Majumder and B. Muller, Phys. Rev. C **74**, 054901 (2006).

[33] R. V. Gavai and S. Gupta, Phys. Rev. D **67**, 034501 (2003).

[34] R. V. Gavai and S. Gupta, Phys. Rev. D **71**, 114014 (2005).

[35] J. O. Andersen, S. Mogliacci, N. Su, and A. Vuorinen, Phys. Rev. D **87**, 074003 (2013).

[36] N. Haque, A. Bandyopadhyay, J. O. Andersen *et al.*, J. High Energy Phys. 05 (2014) 027.

[37] P. B. Munzinger, K. Redlich, and J. Stachel, in *Quark Gluon Plasma* (World Scientific, Singapore, 2004), Vol. 3, pp. 491–599 [arXiv:nucl-th/0304013].

[38] J. Beringer, J.-F. Arguin, R. M. Barnett *et al.* (Particle Data Group), Phys. Rev. D **86**, 010001 (2012).

[39] V. Koch, A. Majumder, and J. Randrup, Phys. Rev. Lett. **95**, 182301 (2005).

[40] J.-P. Blaizot, E. Iancu, and A. Rebhan, Phys. Lett. B **523**, 143 (2001).

[41] J. Xu, S. Yu, F. Liu, and X. Luo, Phys. Rev. C **94**, 024901 (2016).

[42] A. Chatterjee *et al.*, J. Phys. G: Nucl. Part. Phys. **43**, 125103 (2016).

[43] X. Luo, Phys. Rev. C **91**, 034907 (2015); J. Phys. G: Nucl. Part. Phys. **39**, 025008 (2012).

[44] G. Maurice and M. A. Kendall, *The Advanced Theory of Statistice*, 2nd ed. (Charles Griffin & Company, London, 1945), Vol. I.